

Research Article

TMT-Based Quantitative Proteomics Analysis of the Fish-Borne Spoiler *Shewanella putrefaciens* Subjected to Cold Stress Using LC-MS/MS

Xin Gao,^{1,2,3,4} Peiyun Li,^{1,2,3,4} Jun Mei ^{1,2,3,4} and Jing Xie ^{1,2,3,4,5}

¹College of Food Science and Technology, Shanghai Ocean University, Shanghai 201306, China

²National Experimental Teaching Demonstration Center for Food Science and Engineering Shanghai Ocean University, Shanghai 201306, China

³Shanghai Engineering Research Center of Aquatic Product Processing and Preservation, Shanghai 201306, China

⁴Shanghai Professional Technology Service Platform on Cold Chain Equipment Performance and Energy Saving Evaluation, Shanghai 201306, China

⁵School of Public Administration and Services, Shanghai Urban Construction Vocational College, Shanghai 201415, China

Correspondence should be addressed to Jun Mei; delightmay@hotmail.com and Jing Xie; jxie@shou.edu.cn

Received 29 August 2020; Revised 4 November 2020; Accepted 26 December 2020; Published 8 January 2021

Academic Editor: Ajaya Kumar Singh

Copyright © 2021 Xin Gao et al. This is an open access article distributed under the Creative Commons Attribution License, which permits unrestricted use, distribution, and reproduction in any medium, provided the original work is properly cited.

Shewanella putrefaciens is a specific spoilage bacterium for fish during cold storage. To better understand the molecular mechanisms of cold stress adaptation of *S. putrefaciens*, tandem mass tag- (TMT-) based quantitative proteomic analysis was performed to detect the effects of cold stress on protein expression profiles in *S. putrefaciens* which had been cultivated at 4°C and 30°C, respectively. A total of 266670 peptide spectrum matching numbers were quantified proteins after data analysis. Of the 2292 proteins quantitatively analyzed, a total of 274 were found to be differentially expressed (DE) under cold stress compared with the nonstress control. By integrating the results of Kyoto Encyclopedia of Genes and Genomes (KEGG) analyses, 9 common KEGG terms were found notable for the cold-responsive proteins. Generally, the DE proteins involved in carbohydrate, amino acid, and fatty acid biosynthesis and metabolism were significantly upregulated, leading to a specific energy conservation survival mode. The DE proteins related to DNA repair, transcription, and translation were upregulated, implicating change of gene expression and more protein biosynthesis needed in response to cold stress.

1. Introduction

Fresh fish is very perishable due to endogenous enzymes and microbial activities, which can result in large economic losses [1]. Indeed, the intrinsic properties of fresh fish are favourable for growth and enzymatic activity of spoilage bacteria, with the consequent off-flavours, off-odours, discoloration, textural changes, and slime formation [2]. Cold storage is widely used to maintain the quality of fish and prolong the shelf life [3, 4]. *Shewanella putrefaciens* is considered as the common specific spoilage organisms (SSOs) in fish during cold storage [5, 6]. *S. putrefaciens* has been reported to be able to use electron acceptors, such as TMAO, instead of oxygen to survive under oxygen or hypoxia conditions. It can produce proteolytic and

lipolytic enzymes broken down proteins and produce various flavour defects to lower the fish quality [7]. In addition, *S. putrefaciens* is a cold-adapted bacterium in refrigerated fish and exhibits many special characteristics and molecular mechanisms that allow them to adapt to the cold stress environment [8, 9].

Some bacteria show a variety of physiological adaptation mechanisms, in order to cope with cold stress, survive, and grow in the cold stress environment. The mechanism is as follows:

- (i) Increased fluidity of cell membranes
- (ii) The freezing point of the aqueous phase in the cytoplasm decreased

- (iii) Macromolecules with enhanced stability
- (iv) Under the effects of cold shock and cold acclimation, the reaction protein of cells to temperature decreases
- (v) Peroxidase, catalase, redox, and superoxide dismutase protect reactive oxygen species
- (vi) Whether the catalytic efficiency is maintained under cold stress and under cold stress [10–14].

Proteomics can provide advanced information on microbial metabolism and mechanisms of adaptation to the cold stress environment, and this knowledge could be useful to reveal the cold-adaptation mechanisms in *S. putrefaciens*. Proteomics techniques have been widely used in microbiology, among which two-dimensional electrophoresis and protein identification are commonly used [15]. Due to its high technical reproducibility, improved proteome coverage, and more confident peptide identification and quantification, proteome analysis based on the tandem mass tag (TMT) is suitable for analyzing the abundance of thousands of proteins in complex biological samples [16, 17]. Some research studies have been performed to determine the proteomics changes of bacteria under cold stress. For example, proteomics methods were used to investigate the quantitative proteomics of *Edwardsiella tarda* in the mid-exponential growth phase at the optimal temperature of 37°C for 24 h and then through the hatch at 4°C for two weeks without vibration. Several key proteins related to DNA synthesis and transcription were significantly upregulated [18]. Similar comprehensive studies for *S. putrefaciens* have yet to be carried out. To provide insight into potential mechanisms underlying the ability of *S. putrefaciens* to grow at a temperature of 4°C, we investigated the whole proteome response of *S. putrefaciens* exposed to cold stress using mass spectrometry.

2. Materials and Methods

2.1. Bacterial Strain and Growth Conditions. Broth cultures of *S. putrefaciens* (ATCC 8071) were prepared as follows: 1 mL aliquots of logarithmic phase grown broth cultures were transferred to 250 mL Erlenmeyer flasks containing 100 mL medium. The flasks were incubated aerobically agitating at 200 rpm, at 30 and 0°C, respectively, until an absorbance (OD600) of 0.4 was attained. Six independent replicates were collected for each sample. The cell pellets prepared by centrifugation of the bacterial culture were resuspended and washed three times with phosphate-buffered saline (PBS).

2.2. Protein Extraction and Quantification. The spoilage cells were resuspended in a 600 L lysis buffer and subjected to high-intensity probe ultrasound in a 200 w ice bath (UP-250S sonicator, Scientz, Ningbo, China). The mixtures were centrifuged at 16000 g at 4°C for 5 min. The supernatant was collected, and the protein concentration was quantified using the bicinchoninic acid method. 10 µg protein samples were added to 5X loading buffer at a rate of 5:1 (V/V), and

then, the mixture was put in the boiling water for 5 min. The purity of proteins was determined by sodium dodecyl sulfate-polyacrylamide gel electrophoresis (SDS-PAGE) on the basis of Hou et al. [19].

2.3. Protein Enzymatic Hydrolysis and Peptide Desalting. 300 µg of each sample and 0.1 M DTT were mixed together. The mixture was heated in the boiling water for 5 min and then cooled to room temperature. Then, 200 µL UA buffer (8 M urea, 150 mM Tris-HCl, pH 8.0) was added to the mixture, and the protein was collected by centrifugation with 10 kDa ultrafiltration centrifuge tube at 12,000 ×g for 15 min. This process was repeated twice. Subsequently, the protein was added with 100 µL IAA (50 mM IAA in UA) and oscillated at 600 rpm for 1 min and centrifuged at 12,000 ×g for 10 min at room temperature in dark. The protein was collected by centrifugation with 10 kDa ultrafiltration centrifuge tube at 12,000 ×g for 15 min, and this procedure was repeated twice.

2.4. TMT Labelling. Desalted peptides were reconstituted in 0.1% FA, and the concentration of peptide was determined with the total protein assay kit (BCA method, Nanjing Jiancheng Bioengineering Institute, Nanjing, China). Peptides were reconstituted in 50 mM 2-hydroxyethyl (pH 8.5) and TMT zero reagent (Thermo Fisher, Waltham, USA) was added from stocks dissolved in 100% anhydrous ACN. The peptide-TMT mixture was incubated for 1 h at 25°C and 400 rpm, and the labelling reaction was stopped by the addition of either 5% hydroxylamine to a final concentration of 0.4% or 8 µL of 1 M Tris, pH 8.0, and incubation for 15 min at 25°C and 400 rpm. Peptide solutions were acidified with 45% (v/v) of 10% FA in 10% ACN prior to drying or directly frozen at 80°C and dried by vacuum centrifugation. For in-depth proteome analyses, peptides derived from Lys-C/trypsin digests of luminal and basal PDX tumors were processed as described in Fang et al. [4] but following the optimized TMT labelling protocol.

Briefly, 300 µg peptides were dissolved in 60 µL of 50 mM HEPES (pH 8.5), and the labelling reaction was started by the addition of 300 µg TMT reagents (15 µL of 56.7 mM (20 µg/µL) TMT stocks). Samples were incubated for 1 h at 25°C and 1,000 rpm, and the labelling reaction was quenched using 5 µL of 5% hydroxylamine (15 min; 25°C; 1,000 rpm). Peptide solutions were pooled, frozen at 80°C, and dried by vacuum centrifugation. Subsequently, TMT-labelled samples were desalted using tC18, RP solid-phase extraction cartridges (Waters Corp.; wash solvent: 0.1% TFA; elution solvent: 0.1% FA in 50% ACN), frozen at –80°C, and dried by vacuum centrifugation. TMT-labelled peptides were fractionated via a high-pH reversed-phase column (Pierce™ High-pH Reversed-Phase Peptide Fractionation Kit, Thermo Fisher). Peptides were pooled into 15 fractions. Enrichment was performed using Ni-nitrilotriacetic acid superflow agarose beads (Qiagen) loaded with iron (III) ions. Subsequently, phosphopeptides were desalted using self-packed StageTips (wash solvent: 0.1% FA; elution solvent: 0.1% FA in 50% ACN), frozen at 80°C, and dried by vacuum centrifugation.

2.5. LC-MS/MS Measurements. Tryptic peptides for one-shot analyses were analyzed on an EASY-nLC 1200 (Thermo Scientific) coupled to a Q Exactive Plus mass spectrometer (Thermo Fisher Scientific). After reconstitution in 0.1% FA, an amount corresponding to 500 ng peptides was injected. Peptides were separated on an analytical column (EASY column, 75 μm \times 45 cm, Thermo Fisher Scientific) applying a flow rate of 300 nL/min and following elution program: 0–2 min: from 5 to 8% solvent B (0.1% formic acid + 98% acetonitrile); 2–42 min: from 8 to 23% solvent B; 42–50 min: from 23 to 40% solvent B; 50–52 min: from 40 to 100% solvent B; and 52–60 min: 100% solvent B, respectively. Mass spectrometers were operated in data-dependent and positive ionization mode. On the Q Exactive Plus, MS1 spectra were recorded at a resolution of 70 k using an automatic gain control (AGC) target value of $1e6$ charges and maximum injection time (maxIT) of 50 ms. After peptide fragmentation via higher energy collisional dissociation, MS2 spectra of up to 10 precursors were acquired at 17.5 k resolution using an AGC target value of $1e5$ and a maxIT of 50.

2.6. Database Searching. MaxQuant: for peptide and TMT titration experiments, peptide identification and quantification were performed using MaxQuant (version 1.6.0.16) with its built-in search engine, Andromeda (15, 16). Tandem mass spectra were searched against UniProt-*S. putrefaciens*-3949-20190409.fasta (3949 entries, downloaded on April 9, 2019).

3. Results and Discussion

3.1. Identification of Proteins by Quantitative Proteomics Analysis. The results of spectrometry in the present research included protein identification, peptide identification, protein quantification, and differential protein classification analysis. A total of 266670 peptide spectrum matching (PSM) numbers, 19483 unique peptides, and 2292 quantified proteins were obtained after data analysis.

The intensity histogram for each sample is shown in Figure 1(a). Figure 1(b) was the box plot of normalized density and represented the box plots of \log_2 protein intensity average for each sample.

3.2. Identification of Proteins and Their Total and Differential Abundances. TMT-based quantitative proteomic analysis was developed to identify, quantify, and statistically verify quantitative differences in protein abundance from *S. putrefaciens* grown at 4°C versus 30°C. The use of this approach ensured that the quantitative differences recorded were reliable, irrespective of the magnitude of the quantitative differences, and provided a robust means of interpreting the biological relevance of the data. A total of six experiments were analyzed by LC-MS/MS. Of these proteins, 274 were significant DE proteins with abundances that changed >1.5-fold (cultivated at 30°C/cultivated at 4°C) and *P* values of <0.05. A total of 189 proteins were upregulated and 85 proteins were downregulated (red and green background colors, respectively, in Table 1).

3.3. Bioinformatics Analysis of DE Proteins Identified by TMT. The upregulated and downregulated DE proteins were annotated by Gene Ontology (GO) with Fisher's exact test to better understand the roles that these proteins may play in cold adaptation. The significantly upregulated and downregulated DE proteins were classified into three categories using GO terms: biological process (BP), cell component (CC), and molecular function (MF). The downregulated DE proteins were clustered into 50 BP terms (the most representative term was "organic substance metabolic process"), 20 CC terms (the most representative term was "cell"), and 18 MF terms (the most representative term was "binding"). Each of the first ten terms in BP, CC, and MF determined based on *P* values is listed in Figure 2.

3.4. Categorization of Differentially Downregulated Ribosomal Proteins (RPs). Ribosomes are thought to act as sensors for the heat and cold shock response networks in bacteria and are involved as signals linking environmental stimulus (temperature) with the increased heat shock gene expression [20]. Numerous studies have shown that RPs have a strong functional role, especially in regulating protein synthesis and maintaining the stability of ribosomal complexes [21]. Among the quantified proteins, 44 RPs were identified including 23 30S RPs and 21 50S RPs. Of the 183 significant DE proteins, 31 RPs were upregulated (14 30S and 17 50S, Figure 3) and 21 RPs were downregulated (6 30S and 15 50S). This result is consistent with the fact that RPs may be important for the correct assembly of rRNA under cold stress. All of these RPs had a significant score based on FC, and the very large number indicates that more RPs were likely downregulated in the cold stress environment.

3.5. Main Energy Source Metabolism Network Analysis. The metabolic network of the main energy sources was established, including the citrate cycle, glycolysis/gluconeogenesis, fatty acid degradation, and main amino acid (valine, leucine, and isoleucine) degradation, to reveal the energy change profiles of *S. putrefaciens* in cold temperature (Figure 4). Some of these energy change profiles contained several proteins, and the preferred upregulated proteins are shown. Overall, 13 proteins were identified and quantified in the constructed energy metabolism network. In total, 6 proteins (46.15%) showed a downregulated trend (FC <1), including 2 tricarboxylic acid cycle, 3 fatty acid degradation, and 3 main amino acid. Fumarate hydratase class I (EC 4.2.1.2) and isovaleryl-CoA dehydrogenase (EC 1.3.8.4) were slightly upregulated ($1.2 < \text{FC} < 1.5$, $P < 0.05$), and phosphoglycerate kinase (EC 2.7.2.3), enolase (EC 4.2.1.11), malate dehydrogenase (EC 1.1.1.37), aconitate hydratase B (EC 4.2.1.3), and acetyl-CoA acetyltransferase (EC 2.3.1.9) were significantly upregulated (FC ≥ 1.5 , $P < 0.05$). In addition, these two enzymes are involved in other metabolic processes, such as fatty acid degradation and degradation of valine, leucine, and isoleucine. In addition, retinal dehydrogenase 1 and 3-ketoacyl coenzyme A thiolase are also involved in the degradation of fatty acids and metabolic processes such as valine, leucine, and isoleucine [22]. In

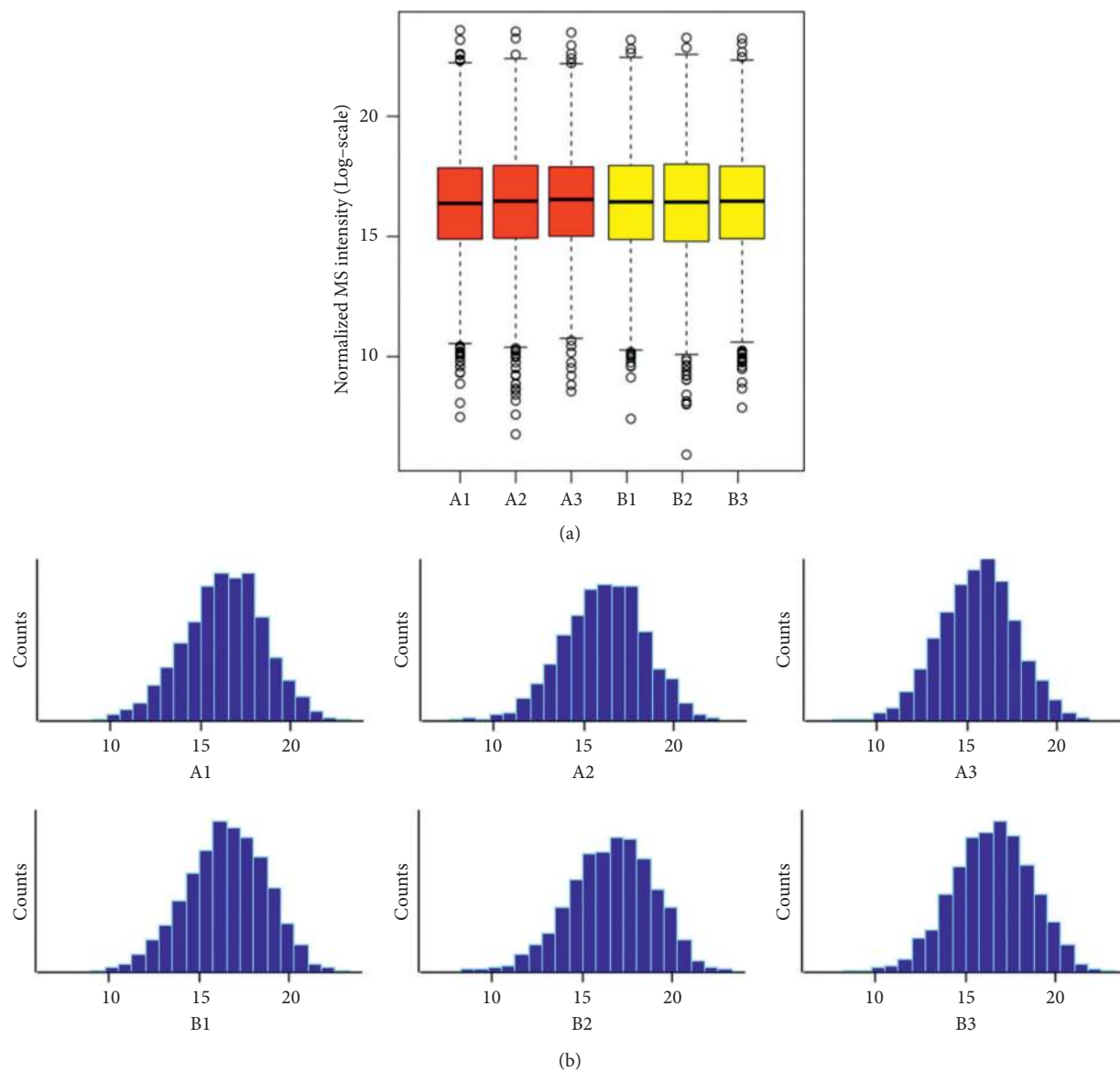


FIGURE 1: (a) Histogram of log₂ protein intensity for each sample. (b) Box plots of log₂ protein (or reporter ion) intensity average for each sample.

summary, amino acid and fatty acid degradation were decreased while glycolysis/gluconeogenesis was activated in *S. putrefaciens* under cold stress.

3.6. Interaction Network of Upregulated DE Proteins.

Studies have shown that proteins in living cells do not exist as a single entity, but rather as functional associations within the cell [23]. It was of great significance to reveal the qualitative characteristics of proteins through the interaction between the formations of the network [24]. By using Cytoscape software against the *S. oneidensis* database, we explored protein interaction networks altered in the cold stress of *S. putrefaciens* by extracting a putative PPI network. According to the filter criteria of score >400, 23 proteins in PPIs showed significantly differential abundance between

S. putrefaciens cultivated at 4°C and 30°C (Figure 5). The proteins were mainly associated with the cellular metabolic process, organonitrogen compound biosynthetic process, plasma membrane ATP synthesis coupled proton transport, protein metabolic process, ATP synthesis coupled proton transport, and ATP biosynthetic process. Among these proteins, 30S and 50S RPs were upregulated, including those encoded by *rpl* and *rps*. Proteins linked to ATP synthase, such as *atpA* and *atpG*, were downregulated significantly. We speculated that these proteins had a pivotal role in the network.

Bacteria may encounter a variety of physiological threats under low temperature stress, such as less and less membrane fluidity, less and less enzyme activity, irregular protein folding, lower and lower ice formation and transcription rate in cells, nutrient transport, translation, cell changes, and

TABLE 1: Detailed information regarding upregulated and downregulated differentially expressed proteins in *S. putrefaciens* cultivated at 4°C and 30°C.

Accession ¹	Sequence length	FC ²	Gene names	Locus	Protein names
Amino acid transport and metabolism					
A4Y849	505	0.52		Sputcn32_2411	L-Lysine 6-monooxygenase, EC 1.14.13.59
A4Y315	797	0.61		Sputcn32_0617	Bifunctional aspartokinase/homoserine dehydrogenase (includes aspartokinase, EC 2.7.2.4; homoserine dehydrogenase, EC 1.1.1.3)
A4Y550	456	0.70		Sputcn32_1355	Zinc metalloprotease, EC 3.4.24.-
A4Y4D8	451	0.72		Sputcn32_1093	L-Glutamine synthetase, EC 6.3.1.2
A4YC19	582	0.80		Sputcn32_3795	Urocanate reductase, EC 1.3.99.33
A4Y7I3	1614	0.82		Sputcn32_2195	Glutamate dehydrogenase, EC 1.4.1.2
A4Y7Q7	939	1.20		Sputcn32_2269	2-Oxoglutarate dehydrogenase E1 component, EC 1.2.4.2
A4Y4E5	425	1.22		Sputcn32_1100	4-Aminobutyrate aminotransferase, EC 2.6.1.19
A4Y656	234	1.28		Sputcn32_1714	3-Oxoacid CoA-transferase, A subunit, EC 2.8.3.5
A4Y1J0	679	1.31		Sputcn32_0087	Oligopeptidase A, EC 3.4.24.70
A4Y3F6	358	1.32	alr	Sputcn32_0759	Alanine racemase, EC 5.1.1.1
A4Y661	389	1.35		Sputcn32_1719	Isovaleryl-CoA dehydrogenase, EC 1.3.8.4
A4Y4D3	285	1.39		Sputcn32_1088	3-Mercaptopyruvate sulfurtransferase, EC 2.8.1.2
A4Y657	315	1.42		Sputcn32_1715	Hydroxymethylglutaryl-CoA lyase, EC 4.1.3.4
A4Y3U2	189	1.43		Sputcn32_0896	Alkyl hydroperoxide reductase C, EC 1.11.1.15
A4Y2I9	524	1.44		Sputcn32_0440	Histidine ammonia-lyase, EC 4.3.1.3
A4Y540	274	1.45	dapD	Sputcn32_1345	2,3,4,5-Tetrahydropyridine-2,6-dicarboxylate N-succinyltransferase, EC 2.3.1.117
A4Y542	278	1.45	map	Sputcn32_1347	Methionine aminopeptidase, EC 3.4.11.18
A4YB15	377	1.46		Sputcn32_3610	Alanine-glyoxylate aminotransferase, EC 2.6.1.44
A4Y342	405	1.46	argD	Sputcn32_0645	Acetylornithine aminotransferase, EC 2.6.1.11
A4YCC5	341	1.47	tdh	Sputcn32_3902	L-Threonine 3-dehydrogenase, EC 1.1.1.103
A4Y3C6	386	1.54		Sputcn32_0729	Methionine gamma-lyase, EC 4.4.1.11
A4Y6M4	344	1.55	astE	Sputcn32_1884	Succinylglutamate desuccinylase, EC 3.5.1.96
A4YCC4	397	1.56	kbl	Sputcn32_3901	2-Amino-3-ketobutyrate coenzyme A ligase, EC 2.3.1.29
A4Y7N9	444	1.61	astB	Sputcn32_2251	N-succinylarginine dihydrolase, EC 3.5.3.23
A4Y1I2	555	1.82	hutU	Sputcn32_0079	Urocanate hydratase, EC 4.2.1.49
A4Y1I0	408	1.85	hutI	Sputcn32_0077	Imidazolonepropionase, EC 3.5.2.7
A4Y1I7	451	1.89		Sputcn32_0084	NADPH-glutathione reductase, EC 1.8.1.7
A4Y596	300	1.89		Sputcn32_1402	3-Hydroxyisobutyrate dehydrogenase, EC 1.1.1.31
A4YAE0	364	1.93	gcvT	Sputcn32_3211	Aminomethyltransferase, EC 2.1.2.10
A4Y6I2	346	2.05		Sputcn32_1670	4-Hydroxyphenylpyruvate dioxygenase, EC 1.13.11.27
A4Y659	288	2.09		Sputcn32_1717	Methylglutaconyl-CoA hydratase, EC 4.2.1.18
A4Y8W2	197	2.18		Sputcn32_2676	Thiol peroxidase, EC 1.11.1.15
A4Y946	370	2.20	aguA	Sputcn32_2760	Putative agmatine deiminase, EC 3.5.3.12
A4Y3Y4	169	2.21	luxS	Sputcn32_0938	S-Ribosylhomocysteine lyase, EC 4.4.1.21
A4Y733	396	2.26		Sputcn32_2045	Aminotransferase, EC 2.6.1.-
A4YAD9	129	2.31	gcvH	Sputcn32_3210	Glycine cleavage system H protein
Carbohydrate transport and metabolism					
A4Y4N4	707	0.66		Sputcn32_1189	Aldehyde ferredoxin oxidoreductase, EC 1.2.7.5
A4Y7R1	131	0.67		Sputcn32_2273	Succinate dehydrogenase subunit C, EC 1.3.5.1
A4Y9V1	594	0.80	opgD	Sputcn32_3021	Glucans biosynthesis protein D
A4Y493	545	1.32	pgi	Sputcn32_1048	Glucose-6-phosphate isomerase, EC 5.3.1.9
A4Y6B4	164	1.41		Sputcn32_1772	4-Hydroxy-4-methyl-2-oxoglutarate aldolase, EC 4.1.1.112
A4Y9A6	404	1.43	deoB	Sputcn32_2820	Phosphopentomutase, EC 5.4.2.7
A4Y566	305	1.49		Sputcn32_1371	N-Acetylglucosamine kinase, EC 2.7.1.59
A4Y6K9	227	1.53		Sputcn32_1869	2-Keto-3-deoxy-phosphogluconate aldolase, EC 4.1.2.14
A4Y579	302	1.60		Sputcn32_1385	UTP--glucose-1-phosphate uridylyltransferase, EC 2.7.7.9
A4Y769	544	1.76	opgG	Sputcn32_2081	Glucans biosynthesis protein G
Cell cycle control, cell division, chromosome partitioning					
A4Y3E0	370	0.73	zapE	Sputcn32_0743	Cell division protein ZapE

TABLE 1: Continued.

Accession ¹	Sequence length	FC ²	Gene names	Locus	Protein names
Cell wall/membrane/envelope biogenesis					
A4Y6J0	192	0.59	rnfA	Sputcn32_1850	Ion-translocating oxidoreductase complex subunit A, EC 7.-.-.-
A4YBG8	460	0.59		Sputcn32_3593	Membrane fusion protein (MFP) family protein
A4Y5V0	178	0.61	pal	Sputcn32_1608	Peptidoglycan-associated protein
A4Y2N5	403	0.69	ftsW	Sputcn32_0486	Probable peptidoglycan glycosyltransferase FtsW, EC 2.4.1.129
A4YB04	244	0.70	zapD	Sputcn32_3427	Cell division protein ZapD
A4Y378	330	0.71		Sputcn32_0681	Mg ²⁺ transporter protein, CorA family protein
A4Y3B5	186	0.75	lptC	Sputcn32_0718	Lipopolysaccharide export system protein LptC
A4Y8T7	395	0.77	bamB	Sputcn32_2649	Outer-membrane protein assembly factor BamB
A4Y3B6	183	1.72		Sputcn32_0719	3-Deoxy-D-manno-octulosonate 8-phosphate phosphatase KdsC, EC 3.1.3.45
A4YBR9	197	1.78	gmhA	Sputcn32_3694	Phosphoheptose isomerase, EC 5.3.1.28
Energy production and conversion					
A4Y920	320	0.58	thrB	Sputcn32_2734	Homoserine kinase, EC 2.7.1.39
A4Y6S9	334	0.62	ruvB	Sputcn32_1939	Holliday junction ATP-dependent DNA helicase RuvB, EC 3.6.4.12
A4Y398	545	0.68	groL groEL	Sputcn32_0701	60 kDa chaperonin
A4Y7T7	637	0.68	htpG	Sputcn32_2299	Chaperone protein HtpG
A4YCH7	142	0.68	atpC	Sputcn32_3955	ATP synthase epsilon chain (ATP synthase F1 sector epsilon subunit) (F-ATPase epsilon subunit)
A4YCH9	286	0.69	atpG	Sputcn32_3957	ATP synthase gamma chain
A4Y6J2	668	0.69	uvrB	Sputcn32_1852	UvrABC system protein B, protein UvrB
A4Y3P6	410	0.69	nqrB	Sputcn32_0850	Na (+)-translocating NADH-quinone reductase subunit B, Na (+)-NQR subunit B, Na (+)-translocating NQR subunit B, EC 7.2.1.1
A4Y2C0	470	0.70	ntrC	Sputcn32_0371	DNA-binding transcriptional regulator NtrC
A4Y4K2	596	0.70	lepA	Sputcn32_1157	Elongation factor 4, EF-4, EC 3.6.5.n1
A4YBH4	670	0.73	rep	Sputcn32_3599	ATP-dependent DNA helicase Rep, EC 3.6.4.12
A4YAH6	604	0.73	dsbD	Sputcn32_3247	Thiol:disulfide interchange protein DsbD, EC 1.8.1.8
A4Y3F5	468	0.74		Sputcn32_0758	Replicative DNA helicase, EC 3.6.4.12
A4YCH8	463	0.75	atpD	Sputcn32_3956	ATP synthase subunit beta, EC 7.1.2.2
A4YAV2	722	0.75		Sputcn32_3373	DNA helicase, EC 3.6.4.12
A4Y1A4	461	0.76	dnaA	Sputcn32_0001	Chromosomal replication initiator protein DnaA
A4Y934	856	0.76	mutS	Sputcn32_2748	DNA mismatch repair protein MutS
A4YCI0	513	0.76	atpA	Sputcn32_3958	ATP synthase subunit alpha, EC 7.1.2.2
A4Y4B7	429	0.76		Sputcn32_1072	NADH dehydrogenase, EC 1.6.99.3
A4Y675	720	0.77	ppk	Sputcn32_1733	Polyphosphate kinase, EC 2.7.4.1
A4Y965	149	0.77	nrdR	Sputcn32_2779	Transcriptional repressor NrdR
A4YBZ9	319	0.77	birA	Sputcn32_3775	Bifunctional ligase/repressor BirA
A4Y406	274	0.78	hmuV	Sputcn32_0960	Hemin import ATP-binding protein HmuV, EC 7.6.2.-
A4Y9Z6	494	0.78		Sputcn32_3066	NAD(P) transhydrogenase subunit beta, EC 7.1.1.1
A4Y3M4	464	0.79	mpl	Sputcn32_0827	UDP-N-acetylmuramate--L-alanyl-gamma-D-glutamyl-meso-2,6-diaminoheptandioate ligase, EC 6.3.2.45
A4Y9A0	454	0.79	radA	Sputcn32_2814	DNA repair protein RadaA
A4Y2J9	696	0.80	recG	Sputcn32_0450	ATP-dependent DNA helicase RecG, EC 3.6.4.12
A4Y470	857	0.80	clpB	Sputcn32_1024	Chaperone protein ClpB
A4Y8E4	192	0.80	tdk	Sputcn32_2506	Thymidine kinase, EC 2.7.1.21
A4Y9N9	207	0.81		Sputcn32_2957	Corrinoid adenosyltransferase, EC 2.5.1.17
A4Y5P9	602	0.81	msbA	Sputcn32_1557	Lipid A export ATP-binding/permease protein MsbA, EC 7.5.2.6
A4Y427	388	0.82	obg	Sputcn32_0981	GTPase Obg, EC 3.6.5.-
A4Y4E0	378	0.83	potA	Sputcn32_1095	Spermidine/putrescine import ATP-binding protein PotA, EC 7.6.2.11
A4Y8T3	525	1.20	guaA	Sputcn32_2645	GMP synthase (glutamine-hydrolyzing), EC 6.3.5.2
A4YBZ8	316	1.21	coaA	Sputcn32_3774	Pantothenate kinase, EC 2.7.1.33
A4Y8F6	571	1.22	proS	Sputcn32_2518	Proline--tRNA ligase, EC 6.1.1.15
A4Y9M1	1074	1.22	carB	Sputcn32_2939	Carbamoyl-phosphate synthase large chain, EC 6.3.5.5

TABLE 1: Continued.

Accession ¹	Sequence length	FC ²	Gene names	Locus	Protein names
A4Y5H4	556	1.24	glnS	Sputcn32_1482	Glutamine--tRNA ligase, EC 6.1.1.18
A4Y334	640	1.25	deaD	Sputcn32_0637	ATP-dependent RNA helicase DeaD, EC 3.6.4.13
A4YBS3	332	1.25	trpS	Sputcn32_3698	Tryptophan--tRNA ligase, EC 6.1.1.2
A4Y7N1	789	1.25		Sputcn32_2243	Phosphoenolpyruvate synthase, EC 2.7.9.2
A4Y9M2	386	1.29	carA	Sputcn32_2940	Carbamoyl-phosphate synthase small chain, EC 6.3.5.5
A4Y5T8	345	1.32	purM	Sputcn32_1596	Phosphoribosylformylglycinamidine cyclo-ligase, EC 6.3.3.1
A4Y6M8	360	1.33	nadA	Sputcn32_1888	Quinolinate synthase A, EC 2.5.1.72
A4Y545	245	1.34	pyrH	Sputcn32_1350	Uridylate kinase, EC 2.7.4.22
A4Y2N4	439	1.37	murD	Sputcn32_0485	UDP-N-acetylmuramoylalanine--D-glutamate ligase, EC 6.3.2.9
A4Y4H3	397	1.37	tyrS	Sputcn32_1128	Tyrosine--tRNA ligase, EC 6.1.1.1
A4YA38	550	1.37	rhlE	Sputcn32_3108	ATP-dependent RNA helicase RhlE, EC 3.6.4.13
A4Y928	958	1.38	valS	Sputcn32_2742	Valine--tRNA ligase, EC 6.1.1.9
A4Y9Z3	565	1.40	cysI	Sputcn32_3063	Sulfite reductase [NADPH] hemoprotein beta-component, EC 1.8.1.2
A4Y959	323	1.41	thiL	Sputcn32_2773	Thiamine-monophosphate kinase, EC 2.7.4.16
A4Y6G8	327	1.42	pheS	Sputcn32_1828	Phenylalanine--tRNA ligase alpha subunit, EC 6.1.1.20
A4Y7E3	231	1.43	lolD	Sputcn32_2155	Lipoprotein-releasing system ATP-binding protein LolD, EC 7.6.2.-
A4YBL9	292	1.44	prpB	Sputcn32_3644	2-Methylisocitrate lyase, 2-MIC, EC 4.1.3.30
A4Y4A4	940	1.46	ileS	Sputcn32_1059	Isoleucine--tRNA ligase, EC 6.1.1.5
A4Y5I7	401	1.49	fabV	Sputcn32_1495	Enoyl-[acyl-carrier-protein] reductase [NADH], EC 1.3.1.9
A4YA91	317	1.51	gshB	Sputcn32_3162	Glutathione synthetase, EC 6.3.2.3
A4Y7C9	143	1.53	ndk	Sputcn32_2141	Nucleoside diphosphate kinase, EC 2.7.4.6
A4Y6Z5	428	1.55	serS	Sputcn32_2007	Serine--tRNA ligase, EC 6.1.1.11
A4Y9Q3	639	1.60	dnaK	Sputcn32_2971	Chaperone protein DnaK
A4Y2H2	198	1.71	azoR	Sputcn32_0423	FMN-dependent NADH-azoreductase, EC 1.7.1.17
A4YAY0	432	2.11	purD	Sputcn32_3402	Phosphoribosylamine--glycine ligase, EC 6.3.4.13
A4Y3S0	391	2.25	pgk	Sputcn32_0874	Phosphoglycerate kinase, EC 2.7.2.3
A4Y397	96	3.88	groS groES	Sputcn32_0700	10 kDa chaperonin
Lipid transport and metabolism					
A4Y4F4	203	0.54	plsY	Sputcn32_1109	G3P acyltransferase, GPAT, EC 2.3.1.275
A4Y9G1	219	0.70	lipB	Sputcn32_2875	Octanoyltransferase, EC 2.3.1.181
A4Y625	238	0.72	fadR	Sputcn32_1683	Fatty acid metabolism regulator protein
A4Y898	436	0.72	fadI	Sputcn32_2460	3-Ketoacyl-CoA thiolase, EC 2.3.1.16
A4Y553	341	0.75	lpxD	Sputcn32_1358	UDP-3-O-acylglucosamine N-acyltransferase, EC 2.3.1.-
A4Y5S4	248	1.22		Sputcn32_1582	3-Oxoacyl-[acyl-carrier-protein] reductase, EC 1.1.1.100
A4Y4D0	498	1.34		Sputcn32_1085	Aldehyde dehydrogenase (acceptor), EC 1.2.5.2
A4Y7Z3	354	1.38	fabH	Sputcn32_2355	3-Oxoacyl-[acyl-carrier-protein] synthase 3, EC 2.3.1.180
A4Y3G1	245	1.49		Sputcn32_0764	Enoyl-CoA hydratase, EC 4.2.1.17
A4Y5S3	308	1.74		Sputcn32_1581	Malonyl CoA-acyl carrier protein transacylase, EC 2.3.1.39
A4Y883	411	1.83		Sputcn32_2445	3-Oxoacyl-[acyl-carrier-protein] synthase I, EC 2.3.1.41
A4Y5X9	171	2.05	fabA	Sputcn32_1637	3-Hydroxydecanoyl-[acyl-carrier-protein] dehydratase, EC 4.2.1.59
A4Y5S5	77	2.54	acpP	Sputcn32_1583	Acyl carrier protein, ACP
Nucleotide transport and metabolism					
A4Y951	735	0.64		Sputcn32_2765	(P)ppGpp synthetase I, SpoT/RelA, EC 2.7.6.5
A4Y9S5	343	1.32	pyrC	Sputcn32_2994	Dihydroorotase, EC 3.5.2.3
A4Y5T9	208	1.33	upp	Sputcn32_1597	Uracil phosphoribosyltransferase, EC 2.4.2.9
A4Y7I2	339	1.37	pyrD	Sputcn32_2194	Dihydroorotate dehydrogenase, EC 1.3.5.2
A4YAX9	543	1.46	purH	Sputcn32_3401	Bifunctional purine biosynthesis protein PurH (includes phosphoribosylaminoimidazolecarboxamide formyltransferase, EC 2.1.2.3 (AICAR transformylase); IMP cyclohydrolase, EC 3.5.4.10 (ATIC))
A4Y8X8	205	1.49		Sputcn32_2692	dITP/XTP pyrophosphatase, EC 3.6.1.66
A4Y9A7	443	1.54	deoA	Sputcn32_2821	Thymidine phosphorylase, EC 2.4.2.4
A4Y2U2	252	1.55		Sputcn32_0543	Uridine phosphorylase, EC 2.4.2.3

TABLE 1: Continued.

Accession ¹	Sequence length	FC ²	Gene names	Locus	Protein names
A4YCD7	331	1.62	add	Sputcn32_3914	Adenosine deaminase, EC 3.5.4.4
A4Y2C8	103	1.64	ppnP	Sputcn32_0379	Pyrimidine/purine nucleoside phosphorylase, EC 2.4.2.2
A4Y5R0	296	1.71	cdd	Sputcn32_1568	Cytidine deaminase, EC 3.5.4.5
A4Y7B5	245	1.80	kdsB	Sputcn32_2127	8-Amino-3,8-dideoxy-manno-octulosonate cytidyltransferase, EC 2.7.7.90
A4Y7K5	193	1.99	dcd	Sputcn32_2217	dCTP deaminase, EC 3.5.4.13
A4Y726	231	2.08	pyrF	Sputcn32_2038	Orotidine 5'-phosphate decarboxylase, EC 4.1.1.23
A4Y4P9	145	2.97		Sputcn32_1204	Cytosine deaminase, EC 3.5.4.1
Replication, recombination, and repair					
A4Y6I4	213	0.74	nth	Sputcn32_1844	Endonuclease III, EC 4.2.99.18
A4Y5Y2	609	0.82	uvrC	Sputcn32_1640	UvrABC system protein C, protein UvrC
A4Y9F1	343	0.82		Sputcn32_2865	DNA polymerase III, delta subunit, EC 2.7.7.7
A4Y6M1	185	1.24	seqA	Sputcn32_1881	Negative modulator of initiation of replication
A4Y8J7	237	1.24	fliA	Sputcn32_2559	RNA polymerase sigma factor FliA
A4Y729	95	1.43	ihfB himD	Sputcn32_2041	Integration host factor subunit beta, IHF-beta
A4YBK6	92	1.63	rpoZ	Sputcn32_3631	DNA-directed RNA polymerase subunit omega, EC 2.7.7.6
A4Y9D3	158	1.65	greA	Sputcn32_2847	Transcription elongation factor GreA
A4YB05	69	2.50	yacG	Sputcn32_3428	DNA gyrase inhibitor YacG
Secondary metabolites biosynthesis, transport, and catabolism					
A4YAT1	493	0.62	ubiD	Sputcn32_3352	3-Octaprenyl-4-hydroxybenzoate carboxy-lyase, EC 4.1.1.98
A4Y760	222	0.64		Sputcn32_2072	HAD-superfamily hydrolase, subfamily IA, variant 1, EC 3.1.3.18
A4Y3M6	176	0.69		Sputcn32_0829	Hypoxanthine phosphoribosyltransferase, EC 2.4.2.8
A4Y930	418	0.71		Sputcn32_2744	Aspartokinase, EC 2.7.2.4
A4YAL8	289	0.73	psd	Sputcn32_3289	Phosphatidylserine decarboxylase proenzyme, EC 4.1.1.65 (cleaved into phosphatidylserine decarboxylase alpha chain; phosphatidylserine decarboxylase beta chain)
A4Y7Q6	400	0.74		Sputcn32_2268	Dihydrolipoyllysine-residue succinyltransferase component of 2-oxoglutarate dehydrogenase complex, EC 2.3.1.61
A4Y9A3	331	0.75		Sputcn32_2817	Phosphoserine phosphatase, EC 3.1.3.3
A4Y7C7	164	0.76		Sputcn32_2139	Acetolactate synthase, small subunit, EC 2.2.1.6
A4Y719	437	0.79		Sputcn32_2031	Phospholipase D/transphosphatidylase EC 2.7.8.8
A4Y9C6	277	0.82		Sputcn32_2840	Dihydropteroate synthase, EC 2.5.1.15
A4Y2M0	522	1.21	leuA	Sputcn32_0471	2-Isopropylmalate synthase, EC 2.3.3.13
A4Y9M3	270	1.22	dapB	Sputcn32_2941	4-Hydroxy-tetrahydrodipicolinate reductase, EC 1.17.1.8
A4Y9W8	173	1.27		Sputcn32_3038	Protoporphyrinogen oxidase, EC 1.3.3.4
A4Y2M2	474	1.29	leuC	Sputcn32_0473	3-Isopropylmalate dehydratase large subunit, EC 4.2.1.33
A4Y7E1	267	1.31		Sputcn32_2153	Inositol-1-monophosphatase, EC 3.1.3.25
A4Y4A7	318	1.32	ispH	Sputcn32_1062	4-Hydroxy-3-methylbut-2-enyl diphosphate reductase, EC 1.17.7.4
A4Y4T4	440	1.34		Sputcn32_1239	Isocitrate lyase, EC 4.1.3.1
A4Y3R8	664	1.35		Sputcn32_0872	Transketolase, EC 2.2.1.1
A4YAZ4	888	1.39		Sputcn32_3417	Pyruvate dehydrogenase E1 component, EC 1.2.4.1
A4YBI7	619	1.40	ilvD	Sputcn32_3612	Dihydroxy-acid dehydratase, EC 4.2.1.9
A4Y2M1	364	1.42	leuB	Sputcn32_0472	3-Isopropylmalate dehydrogenase, EC 1.1.1.85
A4Y486	163	1.44	purE	Sputcn32_1041	N5-carboxyaminoimidazole ribonucleotide mutase, N5-CAIR mutase, EC 5.4.99.18
A4Y6E8	514	1.48		Sputcn32_1807	Fumarate hydratase class I, EC 4.2.1.2
A4Y4X1	293	1.49		Sputcn32_1276	Farnesyl-diphosphate synthase, EC 2.5.1.10
A4Y5G2	394	1.49		Sputcn32_1470	Glycerate kinase, EC 2.7.1.31
A4Y424	331	1.51		Sputcn32_0978	Trans-hexaprenyltranstransferase, EC 2.5.1.30
A4Y7N3	357	1.54		Sputcn32_2245	Phospho-2-dehydro-3-deoxyheptonate aldolase, EC 2.5.1.54
A4Y591	396	1.55		Sputcn32_1397	Acetyl-CoA acetyltransferase, EC 2.3.1.9
A4YAY7	865	1.58		Sputcn32_3409	Aconitate hydratase B, EC 4.2.1.3
A4Y9W4	217	1.60		Sputcn32_3034	Dihydropteridine reductase, EC 1.5.1.34

TABLE 1: Continued.

Accession ¹	Sequence length	FC ²	Gene names	Locus	Protein names
A4Y670	288	1.63		Sputcn32_1728	Acyl-CoA thioesterase II, EC 3.1.2.2
A4YAE8	311	1.66	mdh	Sputcn32_3219	Malate dehydrogenase, EC 1.1.1.37
A4Y494	318	1.66	tal	Sputcn32_1049	Transaldolase, EC 2.2.1.2
A4YAY4	354	1.68	hemE	Sputcn32_3406	Uroporphyrinogen decarboxylase, EC 4.1.1.37
A4Y5N5	203	1.74	ribA	Sputcn32_1543	GTP cyclohydrolase-2, EC 3.5.4.25
A4Y1D3	302	1.75	hemF	Sputcn32_0030	Oxygen-dependent coproporphyrinogen-III oxidase, EC 1.3.3.3
A4YBS4	226	1.75	gph	Sputcn32_3699	Phosphoglycolate phosphatase, EC 3.1.3.18
A4Y4G4	430	1.77	hemL	Sputcn32_1119	Glutamate-1-semialdehyde 2,1-aminomutase, EC 5.4.3.8
A4Y644	294	1.96	dapA	Sputcn32_1702	4-Hydroxy-tetrahydrodipicolinate synthase, EC 4.3.3.7
A4Y846	278	2.00	trpA	Sputcn32_2408	Tryptophan synthase alpha chain, EC 4.2.1.20
A4YBG2	310	2.04	hemC	Sputcn32_3587	Porphobilinogen deaminase, EC 2.5.1.61
A4Y7T5	214	2.14	adk	Sputcn32_2297	Adenylate kinase, EC 2.7.4.3
A4Y1E3	514	2.14	gpmI	Sputcn32_0040	2,3-Bisphosphoglycerate-independent phosphoglycerate mutase, EC 5.4.2.12
A4Y881	338	2.14	asd	Sputcn32_2443	Aspartate-semialdehyde dehydrogenase, EC 1.2.1.11
A4Y9L3	220	2.15	rpiA	Sputcn32_2931	Ribose-5-phosphate isomerase A, EC 5.3.1.6
A4Y966	417	2.21	glyA	Sputcn32_2780	Serine hydroxymethyltransferase, SHMT, EC 2.1.2.1
A4Y3V1	597	2.22		Sputcn32_0905	Fumarate reductase flavoprotein subunit, EC 1.3.5.4
A4Y452	292	2.27		Sputcn32_1006	Cysteine synthase, EC 2.5.1.47
A4Y943	431	2.31	eno	Sputcn32_2757	Enolase, EC 4.2.1.11
A4Y7M6	344	2.41		Sputcn32_2238	Leucine dehydrogenase, EC 1.4.1.9
Transcription					
A4Y9B8	318	0.63	truB	Sputcn32_2832	tRNA pseudouridine synthase B, EC 5.4.99.25
A4Y9L4	396	0.79	rlmI	Sputcn32_2932	Ribosomal RNA large subunit methyltransferase I, EC 2.1.1.191
A4Y9C1	499	1.27	nusA	Sputcn32_2835	Transcription termination/antitermination protein NusA
A4YB21	101	1.31	fis	Sputcn32_3444	DNA-binding protein Fis
A4Y2K5	237	1.31	rph	Sputcn32_0456	Ribonuclease PH, EC 2.7.7.56
A4Y960	134	1.66	nusB	Sputcn32_2774	Transcription antitermination protein NusB
Translation, ribosomal structure, and biogenesis					
A4Y5U6	228	0.67	tolQ	Sputcn32_1604	Tol-Pal system protein TolQ
A4Y7L6	102	0.70	clpS	Sputcn32_2228	ATP-dependent Clp protease adapter protein ClpS
A4YBZ6	123	0.71	secE	Sputcn32_3772	Protein translocase subunit SecE
A4YA83	697	0.73	fusA	Sputcn32_3154	Elongation factor G, EF-G
A4Y1K1	281	0.73	rlmJ	Sputcn32_0098	Ribosomal RNA large subunit methyltransferase J, EC 2.1.1.266
A4YBY2	201	0.73	rplD	Sputcn32_3758	50S ribosomal protein L4
A4Y836	291	0.75		Sputcn32_2398	Pseudouridine synthase, EC 5.4.99.-
A4YCI2	156	0.76	atpF	Sputcn32_3960	ATP synthase subunit b
A4YBX7	230	0.78	rpsC	Sputcn32_3753	30S ribosomal protein S3
A4YCI4	273	0.78	atpB	Sputcn32_3962	ATP synthase subunit a
A4Y8B9	315	0.79	secF	Sputcn32_2481	Protein-export membrane protein SecF
A4Y8C1	110	0.79	yajC	Sputcn32_2483	Sec translocon accessory complex subunit YajC
A4Y4K5	338	0.80	era	Sputcn32_1160	GTPase Era
A4YBY4	103	1.26	rpsJ	Sputcn32_3760	30S ribosomal protein S10
A4Y4S7	174	1.31	bamE	Sputcn32_1232	Outer-membrane protein assembly factor BamE
A4YBV9	206	1.32	rpsD	Sputcn32_3735	30S ribosomal protein S4
A4Y3E7	246	1.33	rlmB	Sputcn32_0750	23S rRNA (guanosine-2'-O-)-methyltransferase RlmB, EC 2.1.1.185
A4YBW1	118	1.41	rpsM	Sputcn32_3737	30S ribosomal protein S13
A4Y3E1	142	1.42	rplM	Sputcn32_0744	50S ribosomal protein L13
A4Y9C2	151	1.42	rimP	Sputcn32_2836	Ribosome maturation factor RimP
A4YBW4	144	1.44	rplO	Sputcn32_3740	50S ribosomal protein L15
A4Y544	283	1.45	tsf	Sputcn32_1349	Elongation factor Ts, EF-Ts
A4YBW0	130	1.47	rpsK	Sputcn32_3736	30S ribosomal protein S11
A4Y3E2	130	1.49	rpsI	Sputcn32_0745	30S ribosomal protein S9
A4Y705	143	1.56	infC	Sputcn32_2017	Translation initiation factor IF-3
A4Y6A5	85	1.57	minE	Sputcn32_1763	Cell division topological specificity factor
A4Y3F3	150	1.61	rplI	Sputcn32_0756	50S ribosomal protein L9
A4YBX9	92	1.67	rpsS	Sputcn32_3755	30S ribosomal protein S19

TABLE 1: Continued.

Accession ¹	Sequence length	FC ²	Gene names	Locus	Protein names
A4YBY8	124	1.71	rpsL	Sputcn32_3764	30S ribosomal protein S12
A4YBV7	131	1.72	rplQ	Sputcn32_3733	50S ribosomal protein L17
A4YBW5	60	1.72	rpmD	Sputcn32_3741	50S ribosomal protein L30
A4Y5S0	56	1.75	rpmF	Sputcn32_1578	50S ribosomal protein L32
A4Y9F3	109	1.77	rsfS	Sputcn32_2867	Ribosomal silencing factor RsfS
A4Y9B7	89	1.84	rpsO	Sputcn32_2831	30S ribosomal protein S15
A4YBY7	156	1.86	rpsG	Sputcn32_3763	30S ribosomal protein S7
A4Y704	64	1.87	rpmI	Sputcn32_2016	50S ribosomal protein L35
A4Y7L4	72	1.90	infA	Sputcn32_2226	Translation initiation factor IF-1
A4Y426	84	1.90	rpmA	Sputcn32_0980	50S ribosomal protein L27
A4Y4L3	83	1.90	rpsP	Sputcn32_1168	30S ribosomal protein S16
A4YBM9	73	1.92	zapB	Sputcn32_3654	Cell division protein ZapB
A4YBX6	136	1.93	rplP	Sputcn32_3752	50S ribosomal protein L16
A4Y6L5	186	1.96	efp	Sputcn32_1875	Elongation factor P, EF-P
A4Y3F2	75	2.05	rpsR	Sputcn32_0755	30S ribosomal protein S18
A4Y4A1	88	2.09	rpsT	Sputcn32_1056	30S ribosomal protein S20
A4Y5V1	249	2.09	cpoB	Sputcn32_1609	Cell division coordinator CpoB
A4Y6Z8	208	2.14	lolA	Sputcn32_2010	Outer-membrane lipoprotein carrier protein
A4YB74	154	2.17	trmL	Sputcn32_3498	tRNA (cytidine (34)-2'-O)-methyltransferase, EC 2.1.1.207
A4YBX8	110	2.21	rplV	Sputcn32_3754	50S ribosomal protein L22
A4YBX2	104	2.22	rplX	Sputcn32_3748	50S ribosomal protein L24
A4Y2V2	79	2.28	rpmE	Sputcn32_0553	50S ribosomal protein L31
A4Y546	185	2.28	frr	Sputcn32_1351	Ribosome-recycling factor, RRF
A4YBW7	116	2.44	rplR	Sputcn32_3743	50S ribosomal protein L18
A4YBX0	101	2.61	rpsN	Sputcn32_3746	30S ribosomal protein S14
A4Y703	118	2.62	rplT	Sputcn32_2015	50S ribosomal protein L20
A4Y2L3	57	3.30	rpmG	Sputcn32_0464	50S ribosomal protein L33
A4Y5X8	58	3.61	rmf	Sputcn32_1636	Ribosome modulation factor, RMF
A4YCM5	45	3.83	rpmH	Sputcn32_4005	50S ribosomal protein L34
A4YBW2	37	4.44	rpmJ	Sputcn32_3738	50S ribosomal protein L36
Not assigned					
A4Y655	218	1.41		Sputcn32_1713	Butyryl-CoA:acetate CoA transferase, EC 2.8.3.8

¹UniProt and NCBI database accession numbers. ²Average ratio from three replicates by TMT experiment. A protein species was considered differentially accumulated if it exhibited a fold change >1.5-fold (cultivated at 4°C/cultivated at 30°C) with a *P* value of <0.05.

even division [25, 26]. To overcome these challenges, bacteria employ several cold-adaptation strategies such as ensuring nutrient uptake, maintaining the integrity of membrane structure, retaining ribosome functionality, and facing inefficient, slowing protein folding, decreasing the ability in DNA replication and transcription and in RNA translation [27, 28]. Moreover, cold stress affects the membrane fluidity, thus leading the cells to counteract by crafting their membrane lipid composition [26]. Furthermore, bacteria under cold stress protect their DNA, and superoxide dismutase (SOD) and catalase (CATALase) are produced in response to oxidative stress in lipids and proteins due to damage at low temperatures [29].

3.7. Energy Metabolism. We detected 6 downregulated proteins and 7 upregulated proteins related to energy metabolism. A significantly higher level of enzymes involved in glycolysis, which may suggest that *S. putrefaciens* under implicates the production of high energy intermediates, such as pyruvate (Figure 3). Upregulation of the key enzymes phosphoglycerate kinase and enolase showed similar results

in glycolysis. Phosphoglycerate kinase is a housekeeping gene referred to carbon metabolism and energy production [26]. There are eight DE proteins participating in phosphoglycerate kinase (PGK, EC 2.7.2.3), glycolysis, and enolase, which were more abundant in *S. putrefaciens* cultivated at 4°C than that at 30°C (*S. putrefaciens* cultivated at 4°C/*S. putrefaciens* cultivated at 30°C >1.5) (Figure 3). Glycolysis was a more active energy-producing pathway in *S. putrefaciens* cultivated at 4°C under nonfavorable temperature, which was also demonstrated by Sun et al. [30]. PGK is found in every domain and in almost all living organisms [31]. It is coded by *pgk* and PGK activity relates to the conversion of ADP + 3-phospho-d-glyceryl phosphate to ATP + 3-phospho-d-glycerate. PGK is one of the oldest “housekeeping” enzymes, which is found in the most ubiquitous three-carbon portion of the best studied and probably the most ancient metabolic pathway—glycolysis, the Embden–Meyerhof–Parnas cycle (fermentation). PGK activity is also present in several other biochemical processes (e.g., Calvin–Benson–Bassham CO₂ fixation cycle = “CBB”) and is often characterized as metabolically essential [32]. Enolase is a rich expression of cytoplasmic protein in many

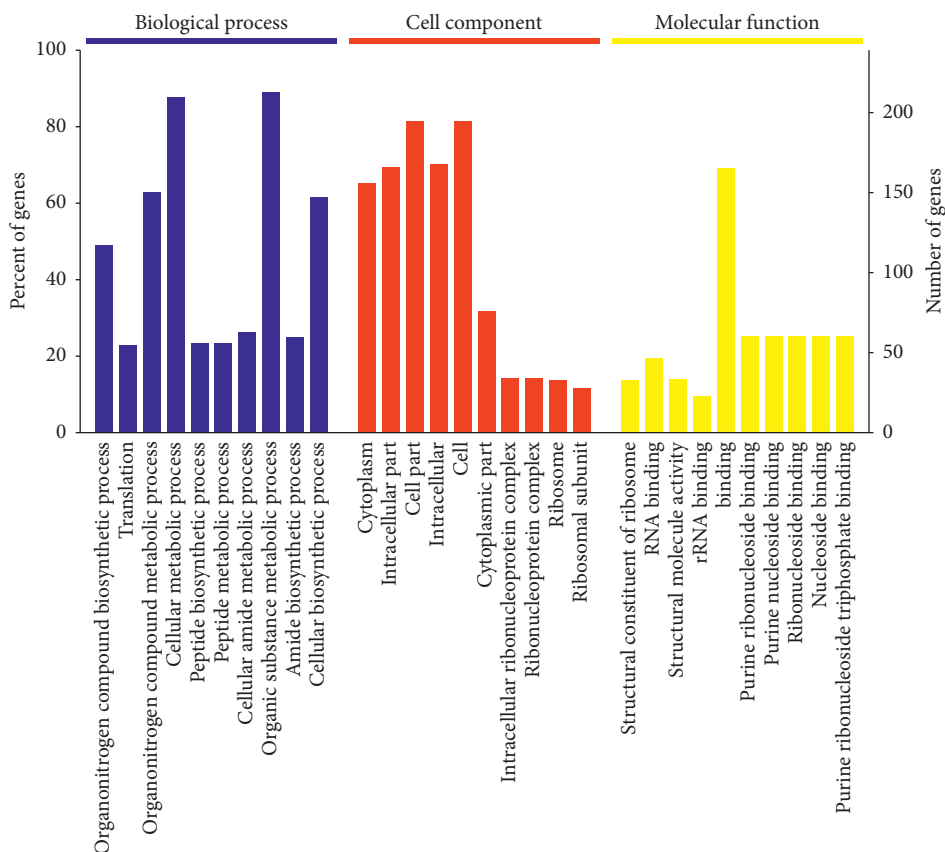


FIGURE 2: Gene Ontology (GO) enrichment analysis of differentially expressed proteins (*S. putrefaciens* cultivated at 4°C and 30°C, respectively). X-axis represented each GO term; Y-axis represented the number of differentially expressed proteins in each category).

organisms. It plays a very important role, especially at the end of the catabolic glycolytic pathway, it is a key glycolytic enzyme, and its main role is to catalyze the dehydration of 2-phosphate-d-glycerol (2-PGA) to produce phosphoenolpyruvate (PEP). In the presence of magnesium ions, it provides energy for organisms, so it is an important energy obtaining way for cells [33]. The upregulation of PGK and enolase was accompanied by the increase of glycolysis rate, which indicates the accumulation of pyruvate.

3.8. RPs. As mentioned above, RPs are one of the most abundant proteins. The effect of cold stress significantly increased their expression (Table 1), indicating their important role in the response to cold stress. Cold stress made the structure of ribosome subunits [34] incomplete, which stalled the translation process and reduced the number of polymers, but this reduction was temporary, accompanied by an increase in the number of a single 70 ribosome and 50 and 30 subunits [15]. Consistent with this, quantities of RPs increased when *S. putrefaciens* was cultivated at 4°C in the current research. For *L. monocytogenes* strains, the strongest and most active genomes are associated with ribosomal genes under cold stress [35]. We observed that nearly all of 30S and 50S RPs were upregulated, including those encoded by rpl, rps, and rpm. The RPs themselves adapt to the new stress conditions [36]. In vitro experiments

showed that the *E. coli* translation apparatus in the cold environment can preferentially act on mRNAs from cold-induced genes [37]. The drop in temperature reduces cell membrane fluidity at the cellular level, and the active transport and secretion of proteins are also affected. The role of RNA helicase in different desiccants was studied. Helicase helps to unlock the secondary structure of RNA so that efficient transcription and translation processes can be achieved under cold stress [38]. Some studies on cold-loving and mesothermal prokaryotes have shown that external ribonuclease and helicase (dead box protein) have this effect; chaperonin proteins have important roles in RNA degradation, nucleotide excision repair pathways, and cold adaptation [39]. There was evidence that RNA degradation under cold stress helps the cells to adapt its RNA metabolism for subsequent growth under cold stress [40]. With the stability of the secondary structure of DNA and RNA, in the case of reduced transcription and translation efficiency and low protein folding efficiency, RPs need to adapt to cold stress in order to function normally [41]. RPs are responsible for ribosome biogenesis and protein translation and play important roles in controlling cell growth, division, and development [42]. In the current research, 47 PRs were identified as being upregulated. The kinetic properties of RPs are different at 4°C than at 30°C, and a large increase in ribosome proteins may lead to the improvement of translation efficiency. Upregulated RPs

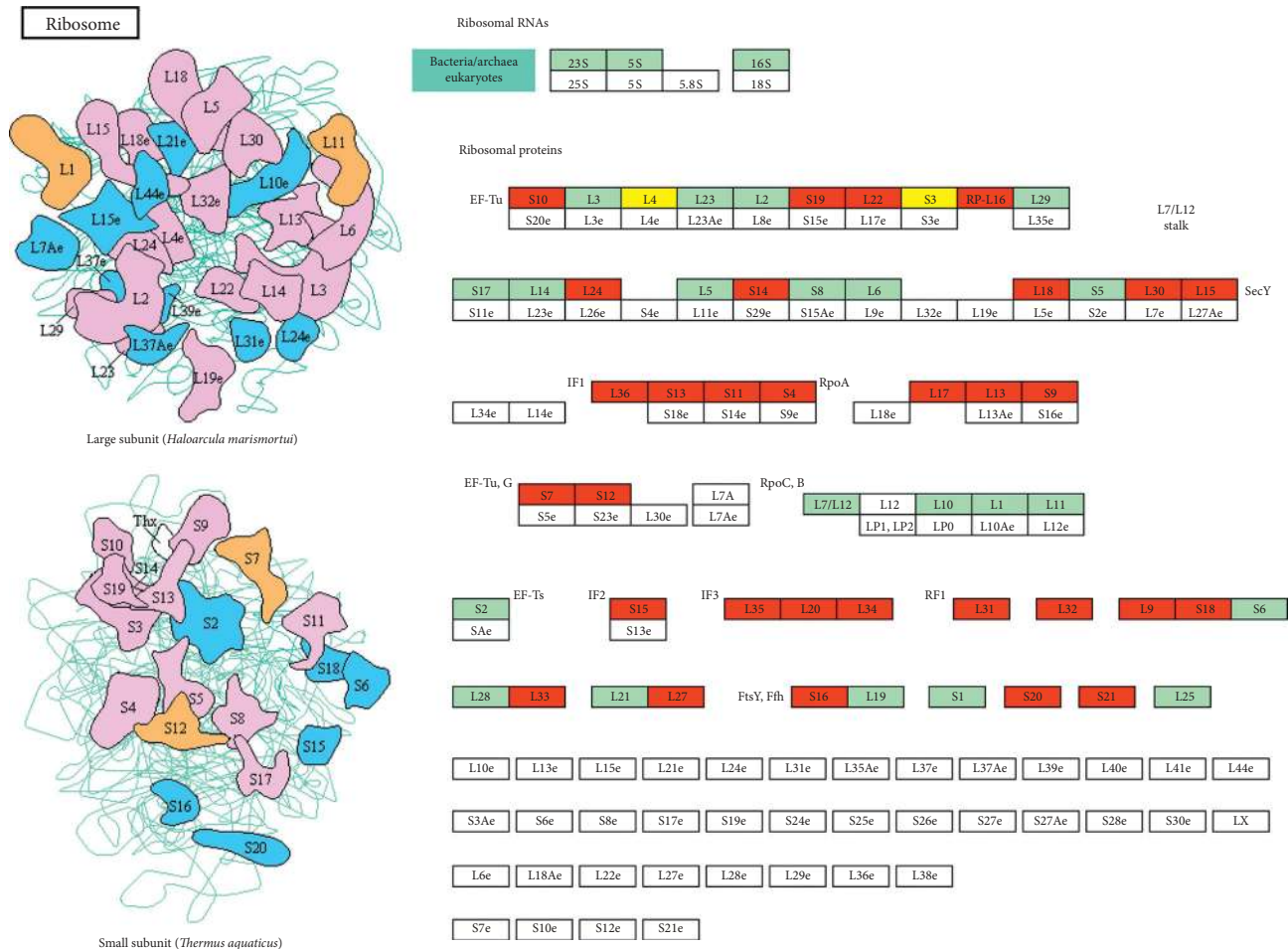


FIGURE 3: Schematic representation of the differentially expressed proteins involved in the ribosome pathway. The red boxes indicate the upregulated proteins, and the green boxes indicate the downregulated proteins.

under cold stress could enhance the appropriate translation or function of ribosome assembly in response to growth requirements. Under this circumstance, ribosomes that are more active under cold stress might be very important for *S. putrefaciens* under cold stress.

3.9. Translation. In the current study, several factors are upregulated under low temperature stress, such as proteins involved in translation (such as initiation factors IF-2 and extension factors), chaperones involved in protein folding, and proteins involved in transcription (such as DNA-directed RNA polymerase) found in *Streptococcus putrefaciens*. This shows that *S. putrefaciens* entered a stabilized phase, which is distinct from the state upon cold shock [15]. In the case of elongation factors, GreA, EF-P, and EF-Ts were upregulated. All were produced at a high level in *S. putrefaciens* under cold stress, indicating that protein synthesis was maintained to live under cold stress. The transcript cleavage factor, GreA, interacts with the RNAP secondary channel and stimulates the intrinsic transcript cleavage activity of RNAP for the removal of the aberrant RNA 3' ends. Therefore, polymerization activity can be restarted from the end of a cleaved RNA allowing transcription to resume [43]. GreA is essential for the survival of

bacteria under stress [44] and it can facilitate RecBCD-mediated resection and inhibits RecA, which plays an important role in impeding DNA break repair in *E. coli* [45], indicating the role of GreA in adapting to the stressful environments. The eukaryotic and archaea extension factor 5A (E/AEF-5A) and its prokaryotic bacterial translation extension factor P (EF-P) would slow the ribosome stagnation. The L-type EF-P is also composed of three bucket domains. Ef-p binds to the polyproline-stalled ribosomes between the peptide-TRNA binding site (P site) and the exiting tRNA (E site) and stimulates the formation of peptide bonds by stabilizing the CCA end of prolyl-TRNA at P site. During translation elongation, the ribosome, with the help of translation elongation factors EF-G, EF-TU, and EF-TS, binds the corresponding amino acid of each codon to the growing polypeptide chain and drives along the coding sequence of the mRNA. Ef-ts are involved in protein synthesis and translation extension, and their expression is increased [46–49].

3.10. Lipid Transport and Metabolism. The effect of temperature on bacterial membrane lipids has been extensively studied [50, 51]. Bacteria adapt their membranes to lower the phase-transition temperature below which their membrane

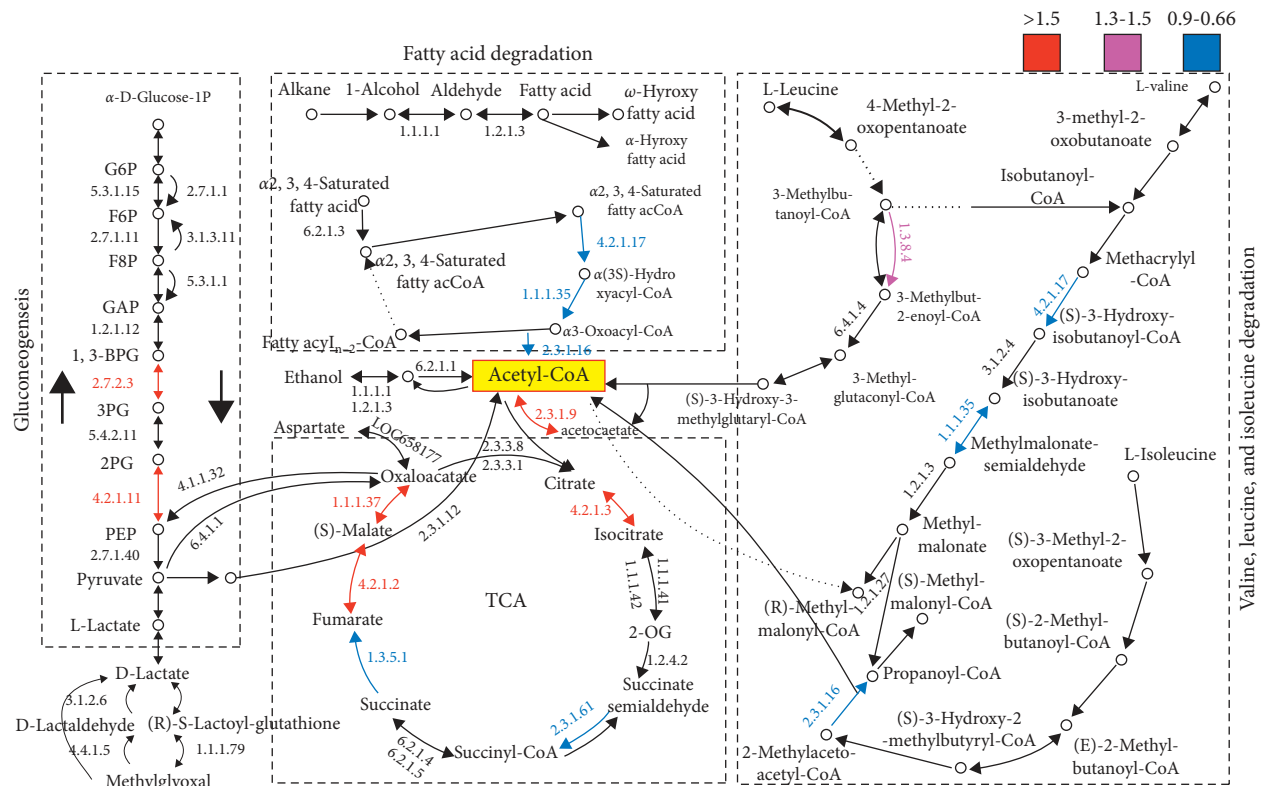


FIGURE 4: The metabolism pathway of the main energy sources. Different colors indicate the ranges of the fold change (cultivated at 4°C/cultivated at 30°C) values.

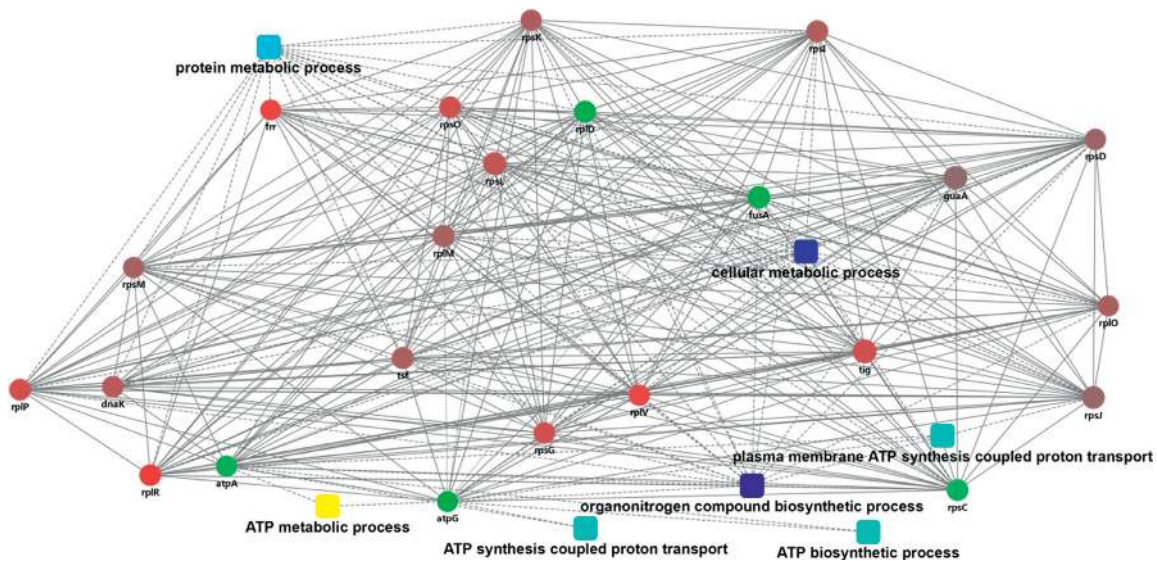


FIGURE 5: PPI network: significantly upregulated differentially expressed proteins of *S. putrefaciens* cultivated at 4°C and 30°C, respectively. The proteins upregulated in *S. putrefaciens* are colored in a gradient color from white to red, $1.52 \leq FC \leq 6.36$.

changes from a “fluid” (liquid-crystalline) to a “rigid” phase to maintain sufficient membrane fluidity under cold stress [52, 53]. In the current research, 13 proteins (5 down-regulated and 8 up-regulated) were associated with lipid transport and metabolism in *S. putrefaciens* under cold stress. PlsY, lipB, fadR, fadI, and lpxD related to the lipid transport and metabolism were downregulated in

S. putrefaciens under cold stress. FadR regulatory protein acts as a regulator controlling bacterial lipid metabolism by inhibiting the fatty acid degradation (fad) system and activating the synthesis of unsaturated fatty acids [54]. In *E. coli*, FadR is a key gene for the synthesis of unsaturated fatty acids and positively regulates fabA and fabB. However, the FadR in *S. putrefaciens* under cold stress only regulates

fabA fatty acid synthesis gene and the fabB protein did not change significantly, which was similar to the result of Yang et al. [54]. Fatty acid degradation occurs through the well-characterized β -oxidation cycle and produces acetyl-CoA, which is further metabolized for energy and precursors of cellular biosynthesis [55]. Acyl-CoA dehydrogenases could catalyze the initial steps in fatty acid β -oxidation. The long-chain fatty acyl-CoA ligase could activate free fatty acids to acyl-CoA thioesters and DE proteins related to lipid synthesis including ketoacyl-ACP synthase III (FabH), which was upregulated under cold stress, which shows the protein expression in *S. putrefaciens* involved in fatty acid elongation and plays a critical role in maintaining the fluidity of membrane [56]. In some research studies, the FabH enzyme of *L. monocytogenes* prefers 2-methylbutyryl-CoA as the precursor of odd-numbered anteiso fatty acids under cold stress and increases the synthesis of anteiso fatty acids [57].

4. Conclusions

The ability to canvass a high proportion of the expressed proteome and define quantitatively large or small changes in protein abundance with strict statistical rigour has provided a strong view of *S. putrefaciens* under cold stress. The proteomics provided functional evidence supporting the importance of specific functional classes of genes that were identified as genomic markers of cold adaptation (e.g., energy metabolism). The quantitative analyses particularly showed the factor in *S. putrefaciens* under cold stress and the study identified specific pathways that were linked to the cold stress environment. The study provides a platform for comparative analyses of cold adaptation of other bacteria.

Data Availability

The data used to support the findings of this study are available from the corresponding author upon request.

Conflicts of Interest

The authors declare that they have no conflicts of interest.

Acknowledgments

This research was financially supported by the National Natural Science Foundation of China (grant numbers 31972142 and 31571914).

References

- [1] H. E. Ramirez-Guerra, F. J. Castillo-Yanez, E. A. Montano-Cota et al., "Protective effect of an edible tomato plant extract/chitosan coating on the quality and shelf life of sierra fish fillets," *Journal of Chemistry*, vol. 2018, Article ID 2436045, 6 pages, 2018.
- [2] M. Sterniša, F. Bucar, O. Kunert, and S. Smole Možina, "Targeting fish spoilers *Pseudomonas* and *Shewanella* with oregano and nettle extracts," *International Journal of Food Microbiology*, vol. 328, Article ID 108664, 2020.
- [3] R. Mabuchi, M. Adachi, A. Ishimaru, H. Zhao, H. Kikutani, and S. Tanimoto, "Changes in metabolic profiles of yellowtail (*Seriola quinqueradiata*) muscle during cold storage as a freshness evaluation tool based on GC-MS metabolomics," *Foods*, vol. 8, no. 10, p. 511, 2019.
- [4] S. Fang, Q. Zhou, Y. Hu, F. Liu, J. Mei, and J. Xie, "Antimicrobial carvacrol incorporated in flaxseed gum-sodium alginate active films to improve the quality attributes of Chinese sea bass (*Lateolabrax maculatus*) during cold storage," *Molecules*, vol. 24, no. 18, p. 3292, 2019.
- [5] P. Li, Z. Chen, M. Tan, J. Mei, and J. Xie, "Evaluation of weakly acidic electrolyzed water and modified atmosphere packaging on the shelf life and quality of farmed puffer fish (*Takifugu obscurus*) during cold storage," *Journal of Food Safety*, vol. 40, Article ID e12773, 2020.
- [6] J. Yan and J. Xie, "Comparative proteome analysis of *Shewanella putrefaciens* WS13 mature biofilm under cold stress," *Front. Microbiol.*, vol. 11, p. 1225, 2020.
- [7] X. Gao, W. Liu, J. Mei, and J. Xie, "Quantitative analysis of cold stress inducing lipidomic changes in *Shewanella putrefaciens* using UHPLC-ESI-MS/MS," *Molecules*, vol. 24, no. 24, p. 4609, 2019.
- [8] M. P. Tribelli and I. N. López, "Reporting key features in cold-adapted bacteria," *Life*, vol. 8, 2018.
- [9] L. Garcia-Descalzo, A. Alcazar, F. Baqueroand, and C. Cid, "Biotechnological applications of cold-adapted bacteria," in *Extremophiles*, pp. 159–174, Wiley, New York, NY, USA, 2012.
- [10] N. Hassan, A. M. Anesio, M. Rafiq et al., "Temperature driven membrane lipid adaptation in glacial psychrophilic bacteria," *Front. Microbiol.*, vol. 11, p. 824, 2020.
- [11] R. A. Baraúna, D. Y. Freitas, J. C. Pinheiro, A. R. C. Foador, and A. A. Silva, "A proteomic perspective on the bacterial adaptation to cold: integrating OMICs data of the psychrotrophic bacterium *exiguobacterium antarcticum* B7," *Proteomes*, vol. 5, no. 9, 2017.
- [12] T. Yu, R. Keto-Timonen, X. Jiang, J.-P. Virtanen, and H. Korkeala, "Insights into the phylogeny and evolution of cold shock proteins: from *Enteropathogenic Yersinia* and *Escherichia coli* to Eubacteria," *International Journal of Molecular Sciences*, vol. 20, no. 16, p. 4059, 2019.
- [13] X. Chen, L. Li, F. Yang, J. Wu, and S. Wang, "Effects of gelatin-based antifreeze peptides on cell viability and oxidant stress of *Streptococcus thermophilus* during cold stage," *Food Chem. Toxicol.*, vol. 136, Article ID 111056, 2020.
- [14] A. Hamdan, "Ecological significance and potential industrial application," *South African Journal of Science*, vol. 114, no. 5/6, Article ID 2017-0254, 2018.
- [15] J. Jia, Y. Chen, Y. Jiang et al., "Proteomic analysis of *Vibrio metschnikovii* under cold stress using a quadrupole Orbitrap mass spectrometer," *Research in Microbiology*, vol. 166, no. 8, pp. 618–625, 2015.
- [16] C. Ma, W. Wang, Y. Wang et al., "TMT-labeled quantitative proteomic analyses on the longissimus dorsi to identify the proteins underlying intramuscular fat content in pigs," *Journal of Proteomics*, vol. 213, Article ID 103630, 2020.
- [17] J. Zecha, S. Satpathy, T. Kanashova et al., "TMT labeling for the masses: a robust and cost-efficient, in-solution labeling approach," *Molecular & Cellular Proteomics*, vol. 18, no. 7, pp. 1468–1478, 2019.
- [18] W. Ma, J. Jia, X. Huang et al., "Stable isotope labelling by amino acids in cell culture (SILAC) applied to quantitative proteomics of *Edwardsiella tarda* ATCC 15947 under prolonged cold stress," *Microbial Pathogenesis*, vol. 125, pp. 12–19, 2018.
- [19] C. Hou, D. Guo, X. Yu, S. Wang, and T. Liu, "TMT-based proteomics analysis of the anti-hepatocellular carcinoma

- effect of combined dihydroartemisinin and sorafenib," *Biomed. Pharmacother.*, vol. 126, Article ID 109862, 2020.
- [20] Y.-H. Han, W.-Z. Liu, Y.-Z. Shi, L.-Q. Lu, S.-D. Xiao, and Q.-H. Zhang, "Gene expression profile of helicobacter pylori in response to growth temperature variation," *The Journal of Microbiology*, vol. 47, no. 4, pp. 455–465, 2009.
- [21] M. K. Thompson, M. F. Rojas-Duran, P. Gangaramani, and W. V. Gilbert, "The ribosomal protein Asc1/RACK1 is required for efficient translation of short mRNAs," *eLife*, vol. 5, Article ID e11154, 2016.
- [22] Z. Xinxin, Y. Shuang, Z. Xunming, W. Shang, Z. Juhong, and X. Jinghui, "TMT-Based quantitative proteomic profiling of overwintering *Lissorhoptus oryzophilus*," *Frontiers in Physiology*, vol. 10, p. 1623, 2020.
- [23] P.-F. Liu, Y. Xia, X.-T. Hua et al., "Quantitative proteomic analysis in serum of *Takifugu rubripes* infected with *Cryptocaryon irritans*," *Fish & Shellfish Immunology*, vol. 104, pp. 213–221, 2020.
- [24] X. C. Zhang, J. Xie, and J. Mei, "Analysis of proteins associated with quality deterioration of grouper fillets based on TMT quantitative proteomics during refrigerated storage," *Molecules*, vol. 24, no. 14, p. 2641, 2019.
- [25] L. Yarzabal, *Antarctic psychrophilic microorganisms and biotechnology: history, current trends, applications, and challenges Microbial Models: From Environmental to Industrial Sustainability*, S. Castro-Sowinski, Ed., vol. 5, pp. 83–118, Springer, Singapore, 2016.
- [26] I. Bharudin, M. F. Abu Bakar, N. H. F. Hashim et al., "Unravelling the adaptation strategies employed by *Glaciomyces antarctica* PI12 on Antarctic sea ice," *Marine Environmental Research*, vol. 137, pp. 169–176, 2018.
- [27] P. Buzzini, E. Branda, M. Goretti, and B. Turchetti, "Psychrophilic yeasts from worldwide glacial habitats: diversity, adaptation strategies and biotechnological potential," *FEMS Microbiology Ecology*, vol. 82, no. 2, pp. 217–241, 2012.
- [28] G. Cacace, M. F. Mazzeo, A. Sorrentino, V. Spada, A. Malorni, and R. A. Siciliano, "Proteomics for the elucidation of cold adaptation mechanisms in *Listeria monocytogenes*," *Journal of Proteomics*, vol. 73, no. 10, pp. 2021–2030, 2010.
- [29] D. P. Blagojevic, G. Gruborljajic, and M. B. Spasic, "Cold defence responses the role of oxidative stress," *Frontiers in Bioscience*, vol. S3, no. 2, pp. 416–427, 2011.
- [30] Q.-L. Sun, Y.-Y. Sun, J. Zhang et al., "High temperature-induced proteomic and metabolomic profiles of a thermophilic *Bacillus manuisensis* isolated from the deep-sea hydrothermal field of Manus Basin," *Journal of Proteomics*, vol. 203, Article ID 103380, 2019.
- [31] M. Wolf, T. Müller, T. Dandekar, and J. D. Pollack, "Phylogeny of Firmicutes with special reference to *Mycoplasma* (*Mollicutes*) as inferred from phosphoglycerate kinase amino acid sequence data," *International Journal of Systematic and Evolutionary Microbiology*, vol. 54, no. 3, pp. 871–875, 2004.
- [32] J. D. Pollack, Q. Li, and D. K. Pearl, "Taxonomic utility of a phylogenetic analysis of phosphoglycerate kinase proteins of Archaea, Bacteria, and Eukaryota: insights by Bayesian analyses," *Molecular Phylogenetics and Evolution*, vol. 35, no. 2, pp. 420–430, 2005.
- [33] H. Li, Y. Huang, J. Wang et al., "Molecular and biochemical characterization of enolase from *Dermanyssus gallinae*," *Gene*, vol. 756, Article ID 144911, 2020.
- [34] T. Tasara and R. Stephan, "Cold stress tolerance of *Listeria monocytogenes*: a review of molecular adaptive mechanisms and food safety implications," *Journal of Food Protection*, vol. 69, no. 6, pp. 1473–1484, 2006.
- [35] J. Durack, T. Ross, and J. Bowman, "Characterisation of the transcriptomes of genetically diverse *Listeria monocytogenes* exposed to hyperosmotic and low temperature conditions reveal global stress-adaptation mechanisms," *PloS One*, vol. 8, pp. 1–15, 2013.
- [36] C. Barria, M. Malecki, and C. M. Arraiano, "Bacterial adaptation to cold," *Microbiology*, vol. 159, no. 12, pp. 2437–2443, 2013.
- [37] A. M. Giuliadori, A. Brandi, C. Gualerzi, and C. Pon, "Preferential translation of cold-shock mRNAs during cold adaptation," *RNA*, vol. 10, no. 2, pp. 265–276, 2004.
- [38] F. Piette, C. Struvay, and G. Feller, "The protein folding challenge in psychrophiles: facts and current issues," *Environmental Microbiology*, vol. 13, no. 8, pp. 1924–1933, 2011.
- [39] G. Cartier, F. Lorieux, F. Allemand, M. Dreyfus, and T. Bizebard, "Cold adaptation in DEAD-box proteins," *Biochemistry*, vol. 49, no. 12, pp. 2636–2646, 2010.
- [40] A.-F. Ghobakhlu, A. Johnston, L. Harris, H. Antoun, and S. Laberge, "Microarray transcriptional profiling of *Arctic Mesorhizobium* strain N33 at low temperature provides insights into cold adaptation strategies," *BMC Genomics*, vol. 16, p. 383, 2015.
- [41] R. Keto-Timonen, N. Hietala, E. Palonen, A. Hakakorpi, M. Lindström, and H. Korkeala, "Cold shock proteins: a minireview with special emphasis on csp-family of *Enteropathogenicyersinia*," *Frontiers in Microbiology*, vol. 7, p. 1151, 2016.
- [42] K. Jastrzebski, K. M. Hannan, E. B. Tchoubrieva, R. D. Hannan, and R. B. Pearson, "Coordinate regulation of ribosome biogenesis and function by the ribosomal protein S6 kinase, a key mediator of mTOR function," *Growth Factors*, vol. 25, no. 4, pp. 209–226, 2007.
- [43] S. Feng, Y. Liu, W. Liang et al., "Involvement of transcription elongation factor GreA in *Mycobacterium* viability, antibiotic susceptibility, and intracellular fitness," *Frontiers in Microbiology*, vol. 11, p. 413, 2020.
- [44] R. K. Jha, S. Udupa, A. K. Rai et al., "Conditional down-regulation of GreA impacts expression of rRNA and transcription factors, affecting *Mycobacterium smegmatis* survival," *Scientific Reports*, vol. 10, p. 5802, 2020.
- [45] P. Sivaramakrishnan, L. A. Sepúlveda, J. A. Halliday et al., "The transcription fidelity factor GreA impedes DNA break repair," *Nature*, vol. 550, no. 7675, pp. 214–218, 2017.
- [46] R. Krafczyk, J. Macošek, P. K. A. Jagtap et al., "Structural basis for earp-mediated arginine glycosylation of translation elongation factor EF-P," *mBio*, vol. 8, no. 5, pp. e01412–01417, 2017.
- [47] K. Hanawa-Suetsugu, S.-I. Sekine, H. Sakai et al., "Crystal structure of elongation factor P from *Thermus thermophilus* HB8," *Proceedings of the National Academy of Sciences*, vol. 101, no. 26, pp. 9595–9600, 2004.
- [48] N. Tiller and R. Bock, "The translational apparatus of plastids and its role in plant development," *Molecular Plant*, vol. 7, no. 7, pp. 1105–1120, 2014.
- [49] A. McLeod, M. Zagorec, M.-C. Champomier-Vergès, K. Naterstad, and L. Axelsson, "Primary metabolism in *Lactobacillus sakei* food isolates by proteomic analysis," *BMC Microbiology*, vol. 10, no. 1, p. 120, 2010.
- [50] G. Seydlova, J. Beranova, I. Bibova et al., "The extent of the temperature-induced membrane remodeling in two closely related *Bordetella* species reflects their adaptation to diverse environmental niches," *Journal of Biological Chemistry*, vol. 292, no. 19, pp. 8048–8058, 2017.

- [51] M. M. Alreshidi, R. H. Dunstan, M. M. Macdonald, N. D. Smith, J. Gottfries, and T. K. Roberts, "Metabolomic and proteomic responses of *Staphylococcus aureus* to prolonged cold stress," *Journal of Proteomics*, vol. 121, pp. 44–55, 2015.
- [52] N. J. Bale, W. I. C. Rijpstra, D. X. Sahonero-Canavesi et al., "Fatty acid and hopanoid adaption to cold in the methanotroph *Methylovulum psychrotolerans*," *Frontiers in Microbiology*, vol. 10, p. 589, 2019.
- [53] M. F. Siliakus, J. Van Der Oost, and S. W. M. Kengen, "Adaptations of archaeal and bacterial membranes to variations in temperature, pH and pressure," *Extremophiles*, vol. 21, no. 4, pp. 651–670, 2017.
- [54] S.-P. Yang, J. Xie, Y. Cheng, Z. Zhang, Y. Zhao, and Y.-F. Qian, "Response of *Shewanella putrefaciens* to low temperature regulated by membrane fluidity and fatty acid metabolism," *Lebensmittel-Wissenschaft & Technologie*, vol. 117, Article ID 108638, 2020.
- [55] S. Jia, H. Hong, Q. Yang et al., "TMT-based proteomic analysis of the fish-borne spoiler *Pseudomonas psychrophila* subjected to chitosan oligosaccharides in fish juice system," *Food Microbiology*, vol. 90, Article ID 103494, 2020.
- [56] Y. Yoon, H. Lee, S. Lee, S. Kim, and K.-H. Choi, "Membrane fluidity-related adaptive response mechanisms of foodborne bacterial pathogens under environmental stresses," *Food Research International*, vol. 72, pp. 25–36, 2015.
- [57] A. K. Singh, Y.-M. Zhang, K. Zhu et al., "FabH selectivity for anteiso branched-chain fatty acid precursors in low-temperature adaptation in *Listeria monocytogenes*," *FEMS Microbiology Letters*, vol. 301, no. 2, pp. 188–192, 2009.